NASA TECHNICAL NOTE

NASA TN D-4977

NASA TN D-4977

RESEARCH PROBLEMS IN ATMOSPHERE ENTRY AND LANDING FOR MANNED PLANETARY MISSIONS

by C. A. Syvertson

Ames Research Center
Moffett Field, Calif.

NATIONAL AERONAUTICS AND SPACE ADMINISTRATION • WASHINGTON, D. C. • JANUARY 1969

RESEARCH PROBLEMS IN ATMOSPHERE ENTRY AND LANDING FOR MANNED PLANETARY MISSIONS

By C. A. Syvertson

Ames Research Center
Moffett Field, Calif.

NATIONAL AERONAUTICS AND SPACE ADMINISTRATION

For sale by the Clearinghouse for Federal Scientific and Technical Information
Springfield, Virginia 22151 – CFSTI price $3.00

RESEARCH PROBLEMS IN ATMOSPHERE ENTRY AND LANDING FOR MANNED PLANETARY MISSIONS*

By C. A. Syvertson

Ames Research Center

SUMMARY

Some of the research problems associated with atmosphere entry for manned planetary missions are assessed with primary emphasis on the problems related to missions to Mars and Venus. The assessment is divided into two parts: First, the requirements associated with entering the Earth's atmosphere are defined, and second, those associated with atmosphere entry and landing at the target planet are considered.

The assessment of the problems of entering the Earth's atmosphere has shown that maximum entry speeds can be expected to range from about 15 to 18 km/sec. The problems of entry at these hyperbolic speeds are then compared with the problems of entering at Apollo's speed of about 11 km/sec. These comparisons include corridor depths, acceleration histories, and convective and radiative heating. From these comparisons it is shown that one major phenomenon distinguishes Earth entry for planetary missions from that for Apollo - a marked increase in radiative heating. The difficulties in estimating the radiative heating of blunt shapes at hyperbolic speeds are discussed. The heat rejection mechanisms available to a thermal protection system are reviewed and the relative importance of each mechanism to the heating environment for hyperbolic entry is compared with that for entry at Apollo speeds. Since the heating environment at hyperbolic speeds is uncertain and since the performance of the thermal protection system itself is also uncertain, effects of these uncertainties on the weight of thermal protection systems are examined.

In the second part of the paper, it is shown that for missions to Mars and Venus the entry speeds are relatively modest, being about 6 to 10 km/sec at Mars and about 11 to 13 km/sec at Venus. For this speed range and for the typical atmospheres suggested for the planets, convective heating does not differ significantly from that in air under corresponding conditions. The radiative heating at lower speeds is somewhat higher than in air, but at speeds near 10 km/sec, it will be similar to that in air at corresponding conditions unless significant amounts of argon are present. It is further shown that one of the primary problems of entering the atmosphere of nearby planets is the terminal landing maneuver on Mars. With the low surface pressures estimated for that planet, very large parachutes deployed at conditions well beyond current experience will be required.

---

*Presented as "Entry and Landing Requirements for Manned Planetary Missions" at AIAA Technology for Manned Planetary Missions Meeting, New Orleans, Louisiana, March 4-6, 1968.

INTRODUCTION

The objective of the present paper is to examine some of the research problems associated with atmosphere entry and landing for manned planetary missions. It is recognized that these missions are well into the future and, in fact, a decision to carry out such missions will not be considered for a number of years. Thus there is ample time to develop in an orderly and economical fashion the knowledge and technology required to carry out these missions. Having adequate time may be a significant advantage since, in many cases, the operational requirements for manned planetary missions represent major advances in technology. In these cases, it is necessary first to examine the operational characteristics of example missions, to assess the technology requirements associated with these characteristics, to compare these requirements with available technology, to define needs for research to provide the indicated advances in technology, to specify the requirements for new facilities for experimental research, and perhaps even to devise new ways to achieve the desired capabilities in test facilities. The process can indeed be a long one and the steps just noted will serve as a general outline for the material that follows.

There are two phases of a manned planetary mission that involve entry and landing - one of these is at the target planet and the other is at Earth return. Both of these phases will be considered, but the latter one, Earth return, will be considered first primarily because the problems for this area are better defined. It can also be argued that a mission must be planned in reverse with first consideration given to the final phase since it will interact with all previous phases.

Since past missions have provided considerable experience in entering and landing in the Earth's atmosphere, the primary questions in this area associated with manned planetary missions are "How much greater are the entry speeds?" and "What new problems will be encountered at these greater speeds?" There is considerably less experience, especially in this country, related to entering and landing in the atmospheres of other planets, but the primary question here would seem to be "What problems are introduced by the differences in structure and composition of the planetary atmospheres?" Before embarking on the discussion that these questions suggest, it is appropriate to mention earlier reviews that provide additional summaries of future entry and landing problems. The papers of Allen,[1,2] Seiff,[3-5] and Roberts[6] as well as several others[7-10] provide useful background for the present subject.

NOTATION

A reference area

B Planck's function

C_D drag coefficient

c_p specific heat at constant pressure

D drag

G resultant acceleration

H enthalpy

h altitude

I_s intensity

I_{sp} specific impulse

L lift

M Mach number

m mass

q heat flux

R gas constant

Re Reynolds number

R_N nose radius

T temperature

V speed

W weight

x longitudinal coordinate measured from bow shock wave toward body surface

α absorption coefficient

δ shock-wave standoff distance

ε emissivity

ν wavelength

ρ density

Ω spherical coordinate

Subscripts

o	reference condition
∞	free stream
E	entry
ℓ	length
s	specific
ν	wavelength

EARTH RETURN

Entry Speeds

Of primary concern when considering the problems of entry at Earth return from a planetary mission is the magnitude of the entry speeds that will be encountered. Fortunately, a large number of mission and trajectory studies have been carried out and from these studies a rather clear picture has emerged defining quite comprehensively the range of Earth entry speeds associated with missions to a number of objectives. Some of the earliest work in this area were the contractor studies funded by the NASA[11-15] and NASA in-house studies.[16,17] Most of these studies concentrated on missions to Venus and especially to Mars. Studies of missions to a wider variety of objectives were considerably less comprehensive.[8] From the earliest work, it was discovered that Earth entry speeds were generally highest when the mission objective was Mars. However, further study of this problem showed that the gravitational field of Venus could be used to alter the interplanetary trajectories between Mars and Earth in such a way that the Earth entry speeds would be reduced significantly. This technique, which became known as the Venus Swingby Mode, was found for a special case in the work of Ross[18] and was investigated more generally by Sohn[19] working with Hornby[20] and by Hollister and Prussing.[21] Deerwester[22] used the swingby mode extensively for optimizing missions and later Deerwester and D'Haem[23] made a systematic study of Mars transfer trajectories using Venus swingbys. From this last study, Earth entry speeds for Mars missions are summarized in figure 1. Earth entry speeds are shown for both direct and swingby transfer trajectories for each mission opportunity from 1980 to 1999. In each case, the left edge of the bar

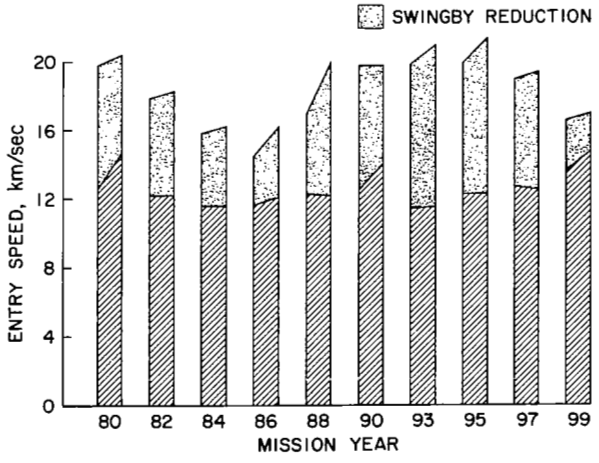

Figure 1.- Earth entry speeds for Mars missions.

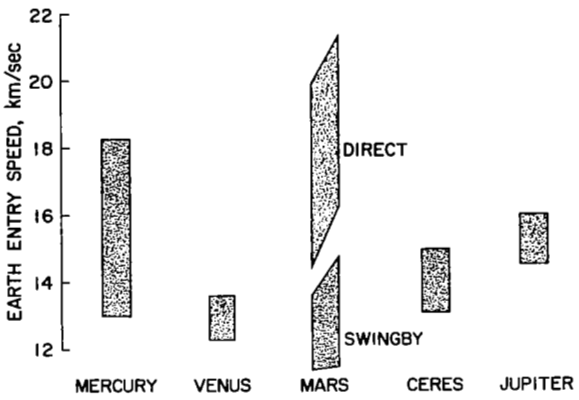

Figure 2.- Earth entry speeds for several mission objectives.

indicates the speeds associated with trajectories optimized assuming the use of atmosphere braking for capture at Mars while the right edge indicates those for trajectories optimized assuming propulsive braking. In both cases, the basis for optimization was to minimize the sum of the velocity increments provided propulsively. The figure effectively summarizes the now well-known result that Venus swingby trajectories reduce the Earth entry speeds for Mars missions by increments of 2 to 8 km/sec. The significance of this reduction is indicated in figure 2 where the range of Earth entry speeds associated with Mars missions is compared with corresponding ranges for other mission objectives. It is apparent that the swingby mode brings the entry speeds for Mars missions into line with those for other objectives. With its use the highest Earth entry speeds are apparently associated with missions to Mercury. The entry speeds for Mercury missions were obtained by Manning[24] who showed that using Venus swingby trajectories also had advantages for Mercury missions, especially if small propulsive maneuvers were allowed near Venus.

The results summarized in figure 2 suggest at least two entry speeds of interest for manned planetary missions. One of these is about 15 km/sec since the capability of entering at this speed will permit a wide variety of trips to Mars, Venus, and the asteroids and even selected trips to other objectives such as Mercury and Jupiter. Another speed of interest is about 18 km/sec since the capability of entering the Earth's atmosphere at this speed would permit a variety of missions to all reasonably nearby objectives. In the material that follows, the problems of entering at these two speeds, 15 and 18 km/sec, will be examined and, for reference purposes, compared to the corresponding problems at Apollo's entry speed of 11 km/sec.

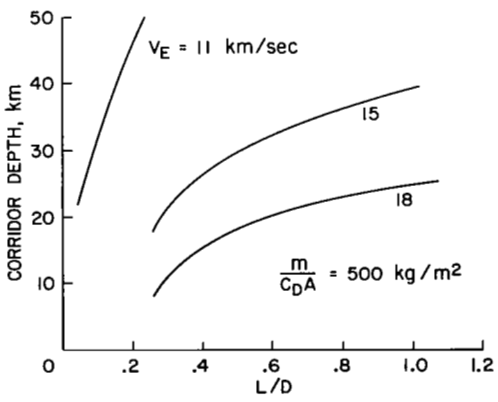

Figure 3.- Entry corridors; G_{max} = 10 g.

Corridors and Accelerations

With the range of entry speeds of interest established, the problem of capture at Earth return can be examined. For this purpose, entry corridors for a maximum acceleration of 10 g are shown in figure 3 as functions of entry vehicle lift-drag ratio for the three entry speeds of 11, 15, and 18 km/sec. At the two higher speeds the corridors are considerably less in depth than those at Apollo's entry speed of 11 km/sec. It is estimated, however, that current guidance

system technology will permit the delivery of the approaching entry vehicle to a corridor approximately 3 km in depth, provided radar tracking from Earth is available.[25] In this event, the lift-drag ratio required for the entry vehicle is relatively modest, being less than 0.3 for entry at the speeds considered. This value can undoubtedly be obtained with reasonably configured vehicles.

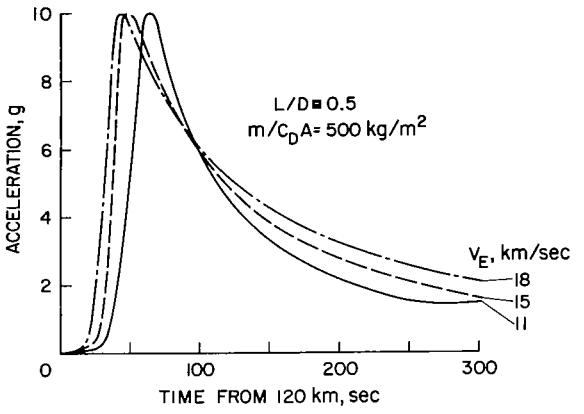

Figure 4.- Acceleration histories.

Acceleration histories for undershoot trajectories that produce a maximum acceleration of 10 g are shown in figure 4. The three entry speeds are, again, 11, 15, and 18 km/sec and in each case the entry vehicle was assumed to have a lift-drag ratio of 0.5 and a drag loading of 500 kg/m^2 (about 100 lb/ft^2 in English units), which are approximately the characteristics of the Apollo command module. With all of the trajectories constrained to give the same maximum acceleration the primary differences are the rates at which the accelerations are imposed. These differences in the acceleration onset rate are not extreme, however, since at 18 km/sec the rate is only about 50 percent greater than for the Apollo entry speed of 11 km/sec. It appears, therefore, that considerations of corridor depth and acceleration for Earth capture will not present major new problems for manned planetary missions.

Heating

The increased entry speeds associated with manned planetary missions will significantly increase entry heating. The magnitude of this increase is indicated in figure 5 where peak convective and radiative heating rates for a blunt body are shown as functions of entry speed.[26,27] The blunt body considered was identical in configuration to Apollo and was assumed to fly at an angle of attack of 33°, giving a lift-drag ratio of 0.5. The results in figure 5 indicate that over the speed range from 11 to 18 km/sec the peak convective heating rate increases by a factor of about 3 but the radiative rate increases by more than an order of magnitude. This increase is due, of course, to the elevated temperatures in the hot gas cap produced by the blunt body's strong bow shock wave. At the higher speeds shown the radiative heating would be even greater, as suggested by the shape of the curve at the lower speeds, if it were not for several alleviating

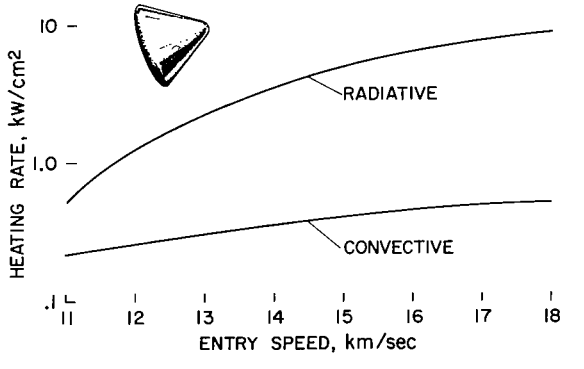

Figure 5.- Peak stagnation-point heating rates; blunt body, L/D = 0.5.

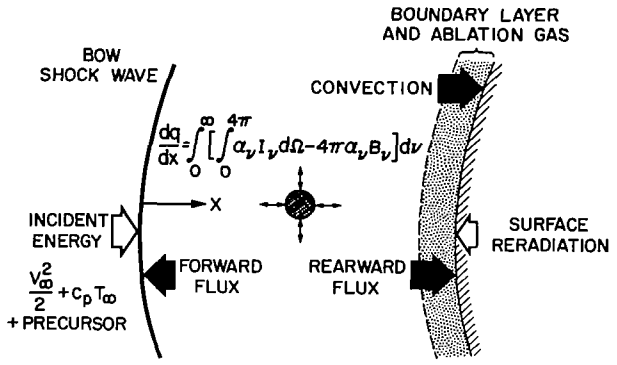

Figure 6.- Transport problem.

phenomena. These phenomena include self-absorption and nonadiabatic effects in the shock layer, and while they tend to limit the radiative heating of blunt entry vehicles, they also complicate considerably the computation of the radiative transport.[28] The one-dimensional transport problem is illustrated schematically in figure 6. From the hot gas cap, heat is convected and radiated rearward to the body but heat is also radiated forward into the oncoming air stream. Some of this forward flux is absorbed by the oncoming stream and thus adds to the enthalpy of the oncoming air. This precursor effect increases the incident energy somewhat[29] and can therefore increase temperature in the gas cap; but at the same time temperatures are lowered as a result of the loss of energy by radiation.[30] To evaluate this nonadiabatic effect as well as the effects of absorption it is necessary to carry out a detailed heat balance on each volume element in the gas cap. The control element in the middle of figure 6 represents one such volume element. The change in heat flux with distance is given by the equation; the first term represents the heat absorbed radiatively by the element, and the second term, that emitted. The heat absorbed by the element depends on the absorption coefficient and the intensity of the incident radiation, both of which are wavelength dependent, and the intensity is spatially dependent so that the incoming flux at each wavelength must be integrated over the spherical surface visible to the element. The emitted radiation is dependent again on the absorption coefficient and upon Planck's function. Since these functions are frequency dependent, an integration must be performed against wavelength. The spectra of the gases are complex, as illustrated in figure 7 for the case of nitrogen[28,31] radiating at 13,000° K. This spectrum has several noteworthy features that provide a convenient device for dividing the radiation into tractable sections. They are the set of UV lines between about 0.1 and 0.2 μ, the set of IR lines near 1 μ, and the underlying continuum radiation. Furthermore, the continuum radiation can be conveniently divided at about 0.12 μ into UV and visual parts. In a later part of this discussion, absorption and nonadiabatic effects on these four parts of the spectrum will be illustrated.

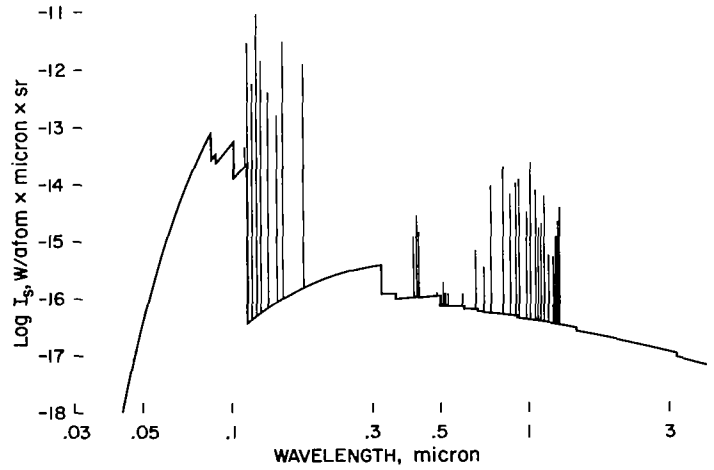

Figure 7.- Typical spectrum; nitrogen, 13,000° K.

Spectra such as the one illustrated in figure 7 are used for the integration noted in figure 6. One typical

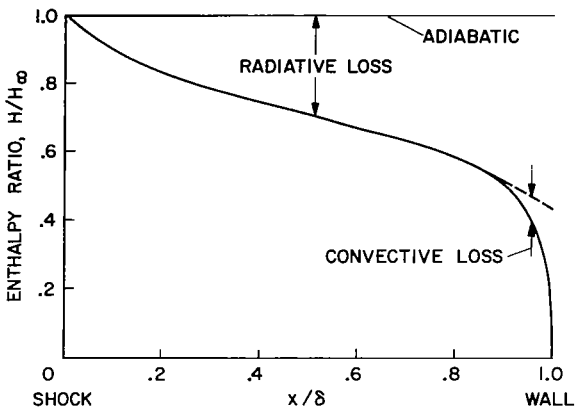

Figure 8.- Energy depletion in shock layer; V_∞ = 16.1 km/sec, h = 60 km, $R_{N_{eff}}$ = 2 m.

result is shown in figure 8 where the enthalpy distribution between the bow shock and the body surface for the stagnation streamline is presented for a blunt body moving at 16.1 km/sec at an altitude of 60 km.[27] For these example conditions, the shock-wave standoff distance would be about 12.7 cm in adiabatic flow; however, cooling of the gas cap with the resulting density increase reduces this distance to slightly less than 10 cm. The cooling due to radiative heat loss is significant as this example shows since this effect reduces the gas enthalpy more than 50 percent near the body. In turn, this loss has a major effect on the radiative emission from the gas as is shown in figure 9 for the same conditions used in figure 8. For each station in the shock layer the two curves indicate the flux transmitted upstream by all the gas downstream of the point and, conversely, the flux transmitted downstream by the gas upstream of the point. The latter curve is the one important to the thermal protection problem. Note that the loss in heat and absorption effects are so significant that the flux is actually decreasing as the flow approaches the body. If the flow were isoenergetic and the gas were optically thin, then the curve representing the downstream flux would be linear and tangent to the curve in figure 9 at the point immediately downstream of the shock (i.e., $x/\delta = 0$). The major significance of the alleviating effects is shown more graphically in figure 10 where the radiative flux to the body estimated with various assumptions is shown. In each case the flux is divided into the contributions of the four components of the spectrum discussed in connection with figure 7. The first bar shows the flux for the adiabatic, optically thin assumption. In this case, the major contributor is the group of UV lines. It was shown in figure 7 that these lines are all below 2000 Å in the vacuum ultraviolet part

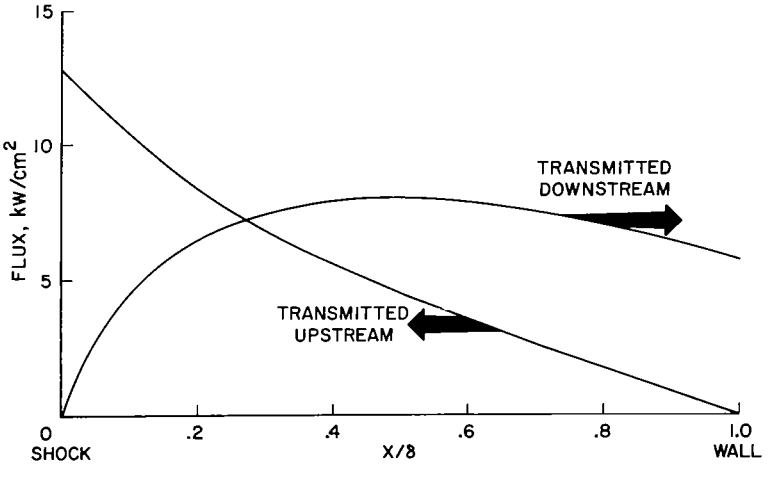

Figure 9.- Transmitted radiative flux; V_∞ = 16.1 km/sec, h = 60 km, δ_o = 12.7 cm.

of the spectrum. This part of the flux is thus heavily absorbed in air. This absorption is clearly evident from the second bar which shows that the flux is reduced more than an order of magnitude by absorption. In many respects the second bar represents a more appropriate reference point from which to start an analysis since the absorption of the UV radiation is well known and use of the unattenuated flux represented by the left bar is quite unrealistic. Comparison of the second and third bars shows again the major effect of energy loss which, for this example, reduces the flux about another order of magnitude. The final bar indicates a rough estimate[28] of the absorption that might result from ablation gases in the boundary layer.** The summary presented in figure 10 shows that the alleviating effects reduce the radiative flux experienced by the body to well below the level available from the energy contained in the oncoming flow. In this example, the flow energy is 72 kW/cm^2 and, in principle, half this energy could be radiated to the body surface.

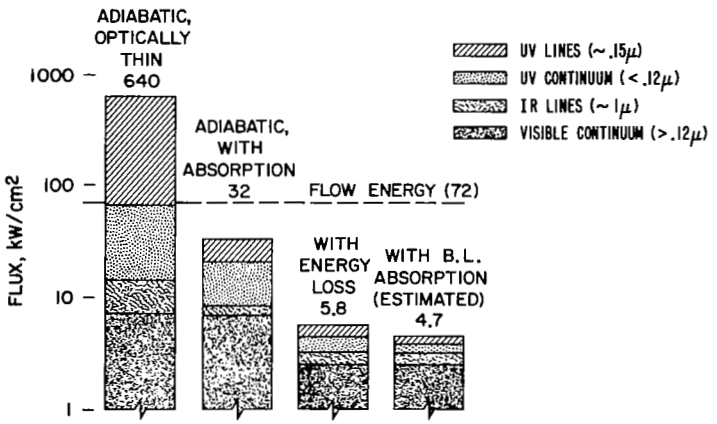

Figure 10.- Summary of radiative heating;
V_∞ = 16.1 km/sec, h = 60 km,
δ_o = 12.7 cm.

The residual flux of about 5 kW/cm^2 in figure 10 is not trivial, since it is many times the heating rates that Apollo will experience on entry; in addition, the fact that the flux is radiative makes thermal protection more difficult. The residual flux level is such that it is still well worthwhile to attempt to avoid it as much as possible. One technique for doing just that has been suggested by Allen, Seiff, and Winovich.[33] Their suggestion is to employ entry vehicles with conical forebodies that produce swept rather than nearly normal shock waves. With the oblique bow shock wave, temperatures in the gas cap are reduced as a result of the reduction in the velocity component normal to the wave. For example, at 18 km/sec and for a bow shock wave of 30° inclination, the radiative heating intensity is less than that behind a normal shock wave at the Apollo entry speed of 11 km/sec. Applications of this approach have been examined in several studies.[34-38]

Configuration Aspects

In order to explore the effects of configuration on heating at hyperbolic speeds the two configurations in figure 11 have been studied in some detail.[36,37] The blunt body is identical in shape to the Apollo entry vehicle. The biconic shape is an application of the principle just discussed along lines first suggested by Shapland.[35] The two configurations have identical lift-drag ratios, volumes, and weights.

**Recent results obtained by Jin H. Chin[32] show that somewhat greater absorption by the ablation gases is possible.

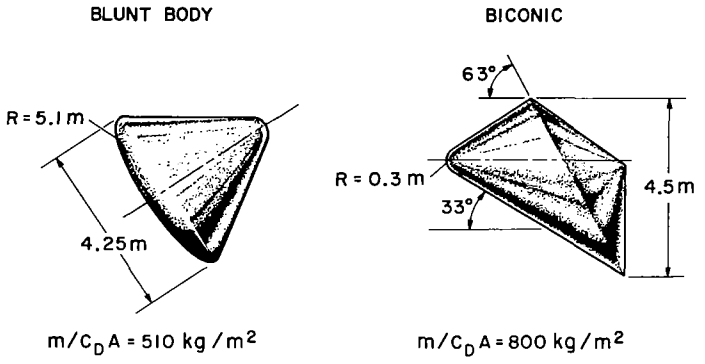

Figure 11.- Shapes studied; L/D = 0.5, vol = 22.8 m^3, m = 7260 kg.

Peak radiative heating rates for an average location on each configuration are shown in figure 12.[38] The average location selected in both cases is at 50 percent of the length of the front face. As the earlier discussion suggested, the conical shape has much lower radiative heating at the selected location. For example, the rate is lower for the biconic at 18 km/sec than it is for the blunt body at 11 km/sec. However, the biconic configuration is not free of radiative heating problems; for example, the peak radiative heating rates for the stagnation points are shown in figure 13. For this location, the rates for the two shapes are essentially identical. This result is rather surprising and it is caused by two effects. First, the nonadiabatic and absorption effects discussed earlier tend to reduce the effects on heating rate of shock-layer thickness and thus nose radius. This trend is suggested by the curves in figure 9 which show that the radiative flux transmitted rearward is nearly constant through about 80 percent of the shock layer. Another cause is the higher drag loading (m/C_DA) of the biconic shape, as noted in figure 11. Because of the higher m/C_DA this shape operates at lower altitude, thus higher air densities, and radiative heating is increased accordingly. The results in figure 13 suggest that the nose radius selected for the biconic shape is too large, although the radius cannot be reduced indefinitely because the reduction would cause a large increase in convective heating. Certainly the results confirm that careful attention must be given to the design of the entry vehicles operating in the environments imposed by entry at speeds approaching 18 km/sec.

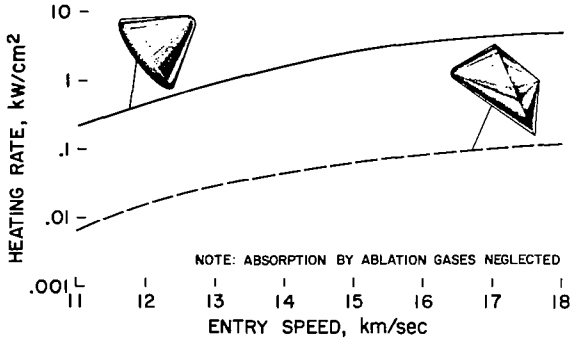

Figure 12.- Peak radiative heating rate; average location.

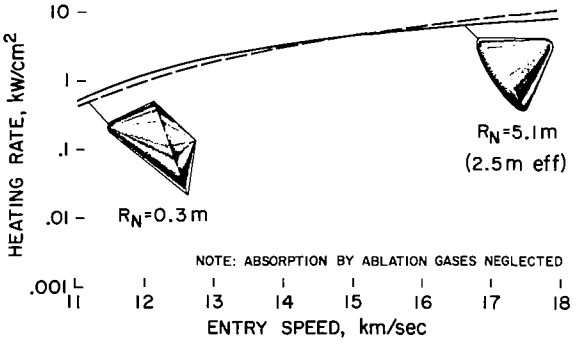

Figure 13.- Peak radiative heating rate; stagnation point.

Thermal Protection

With some understanding of the heating environment, the next problem to be examined is the related one of thermal protection. The mechanisms available to an ablating thermal protection system are indicated in figure 14. The example chosen is that of a charring ablator which is most typical of currently considered systems.[39-41] For this example, there are at least six possible mechanisms. The first encountered by the incident flux is blockage which prevents most of the convective heating from reaching the vehicle surface. It is possible that materials will be found that give off ablation species that will also block appreciable radiative heating by having large absorption coefficients at desired wavelengths. The next mechanism is surface reradiation which can be a significant mechanism for ablators that produce high-carbon chars.[42] If the incoming flux is sufficiently large, the surface temperature will be driven to levels which result in sublimation of the char surface. While this effect limits the amount of heat that can be reradiated, the vaporization process also absorbs heat. In the normal charring ablator, the pyrolysis gases formed at the base of the char percolate through the char and are heated in the process. Consequently, some chemical changes in the gases can occur. From both the heating and the chemical change, more of the incident heat flux is absorbed by an increase in pyrolysis gas enthalpy. The decomposition process at the base of the char which initially produces the pyrolysis gas also absorbs heat. Finally, any heat not absorbed elsewhere must be stored in the solid phase of the virgin material which in this process acts like a simple heat sink.

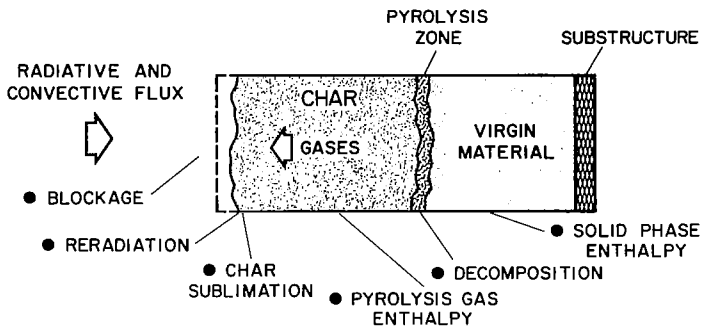

Figure 14.- Thermal protection mechanisms.

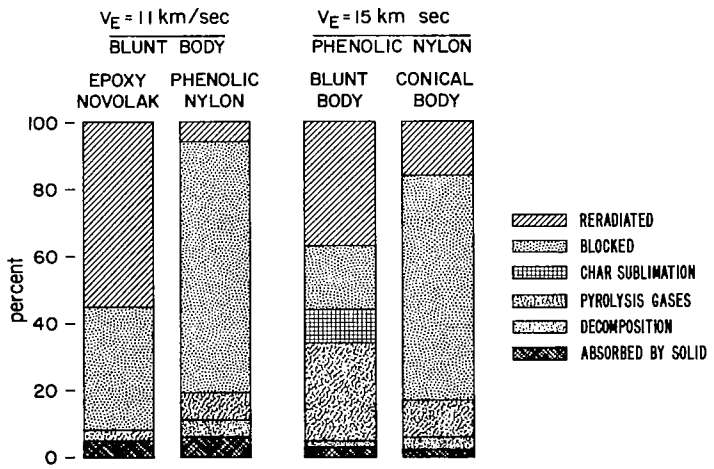

Figure 15.- Heat rejection mechanisms; peak heating, average location.

The relative importance of each of these six processes depends on many factors including the type of material and the characteristics of the incident heating, and, as previously discussed, the heating depends strongly on both entry speed and configuration. The effect of some of these variables on the relative contribution of the various heat rejection mechanisms at peak heating is shown in figure 15. The results are for an average location on an entry body, specifically the same location

considered in figure 12. The left two bars show the effect of differences in material;[43,44] in both cases the results are for a blunt body entering at 11 km/sec (i.e., the Apollo case). For the left bar the material is epoxy novolak in a glass honeycomb, the material used in the Apollo heat shield.[45,46] For the second bar, the material is a high-density phenolic nylon (1.2 gm/cm^3), the material most often considered for use at very high entry speeds. For epoxy novolak, the most important mechanism is surface reradiation; blockage is also very important. Phenolic nylon produces considerably more pyrolysis gas than does epoxy novolak; consequently, blockage plays a much more important, in fact the dominant, role for this material, as is apparent from the second bar. Because of the greater production of gases, both the pyrolysis gas enthalpy and the decomposition contributions are also greater for phenolic nylon.

For this material and the blunt body, there is also a marked change between the results for V_E = 11 km/sec and for 15 km/sec, as can be seen by comparison of the second and third bars. Because of the higher heating rates and the heating being predominantly radiative, several changes occur. First, the relative contribution of blockage is less, in large part because of the change in the heating mechanism. As a result, the surface temperature increases and thus surface reradiation is greater. The surface temperatures are increased to the point that the surface sublimes; thus this mechanism comes into play. In addition, the pyrolysis gases are heated to the higher surface temperature and thus absorb a larger percentage of the heat.

The last bar on the right, in comparison with the third bar, shows the effects of vehicle configuration. This comparison shows the marked differences in heat rejection mechanisms for the blunt and conical shapes. The basic reason for this difference was noted earlier; the use of a conical forebody suppresses the radiative heating at hyperbolic speeds to about the levels associated with a blunt body entering at 11 km/sec (i.e., Apollo). As a result, the rejection mechanisms for a conical body at V_E = 15 km/sec are very similar in their relative importance to those for a blunt body at V_E = 11 km/sec. In fact, this comparison between the second and fourth bars is one of the most interesting and perhaps the most significant of those that can be made in figure 15. It leads to one of the primary conclusions that can be drawn from this study of thermal-protection mechanisms: that the use of a conical forebody on vehicles entering at hyperbolic speeds can result in response by the thermal protection that is similar to current experience. The heating rates and loads are significantly greater as noted earlier, but the designer can use configuration selection to control response of the thermal-protection system.

Vehicle Weights

With some definition of the heating environment and of the characteristics of thermal-protection systems, estimates can be made of the weight of the thermal-protection system[27,37,38] and in turn of the weight of the entry vehicle itself.[9,14] The first of these estimates is shown in figure 16, where heat-shield weights are shown as a function of entry speed. Results are shown for both the blunt and the biconic configurations described in figure 11.

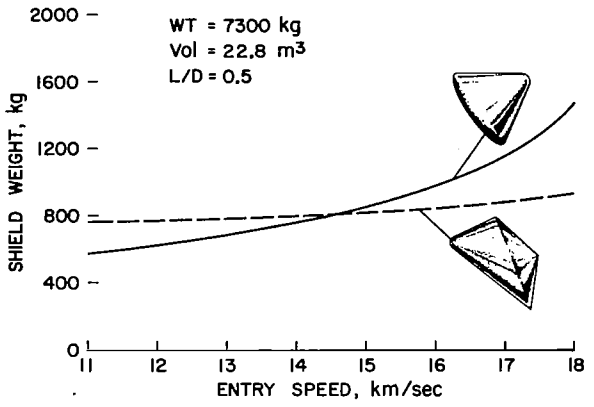

Figure 16.- Heat-shield weights; phenolic nylon.

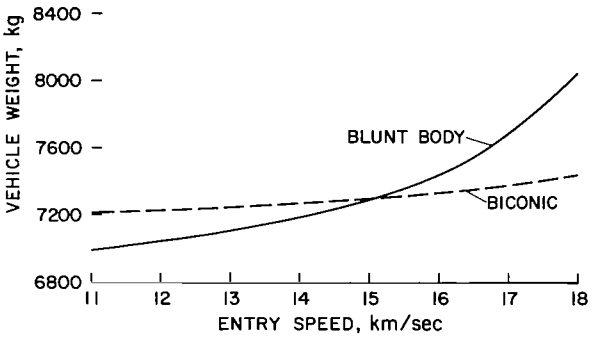

Figure 17.- Earth entry vehicle weights; eight-man crew.

In all cases, the heat-shield material is phenolic nylon; the lift-drag ratio is 0.5; and the weight and volume correspond to about those for an 8-man vehicle.[37, 38] These results reflect the trends suggested in the previous discussion; the weight of the blunt body increases with increasing speed more rapidly than that of the conical body. This trend is a direct ramification of the marked increase in radiative heating and of its effect on the response of the thermal-protection system.

The corresponding total weights of the entry vehicle (fig. 17) were estimated from the results in figure 16 and from the results of earlier work.[14, 37, 38] The trends shown are a direct reflection of those in figure 16. Aside from the effects on thermal protection, increased entry speed in the range from 11 to 18 km/sec should have no major effect on vehicle systems as discussed earlier. Accordingly, in the present analysis, all other system weights were assumed to be independent of entry speed.

Several general observations should be made about the results shown in figures 16 and 17. First, in the speed range from 15 to 18 km/sec the heat shield is estimated to represent between about 10 and 20 percent of the entry vehicle weight. Since the Earth entry vehicle itself may represent only a small part of the weight of a complete spacecraft that departs Earth for a manned planetary mission, the heat-shield weight may not seem significant. A few numbers will tend to negate such a conclusion, however. For example, the results in figure 16 show that the heat shield weighs about 1000 kg. This weight must be carried throughout the mission. Mission and trajectory studies[23] show that each kilogram carried throughout a manned planetary mission can represent between 300 and 1000 kg on the launch pad. On the basis of these numbers, the heat shield may represent some 1000 metric tons of launch vehicle, and such weight, of course, is not negligible. For much the same reason the differences in weight due to configuration shown in figure 17 which at first may seem inconsequential are also important. These differences vary from 200 to 600 kg and thus may represent 200 to 600 metric tons of launch vehicle.

There is one other comment related to the results in figures 16 and 17 that is more important than either of these. All of the results shown are based solely on theoretical analysis. There are essentially no experimental

results with which to confirm these estimates. The absence of such data is especially important because of the wide variations possible in the behavior of the gas in the hot shock layer and in the response of the heat shield to the predicted large heat flux. The foregoing discussions dealing with these problems have served to outline how complex the phenomena are. Obtaining the required data and the necessary experience with the high-temperature gas flows and with suitable ablative materials must be a prime objective in developing the technology for manned planetary missions.

Uncertainty Analyses

The foregoing discussion has served to emphasize the basic uncertainty associated with any weight estimate for the Earth entry speeds of interest for manned planetary missions. In view of the situation it is desirable to examine quantitatively the accuracy of the estimates, particularly those of the heat-shield weight. The weight uncertainties have been analyzed in large part by the Lockheed Missiles and Space Company under contract to the NASA Ames Research Center.[47] Some of the preliminary results of this work have been given in papers by Coleman, Lefferdo, Hearne, and Vojvodich[38] and by Vojvodich.[39] The uncertainties considered in this work are summarized in figure 18. The first perturbation considered was in the radiative flux. The nominal intensities used in the analysis were those published by Wilson and Nicolet.[31] It is difficult to describe briefly the changes considered in the radiative heating; however, it is approximately correct to say that the increase in the flux from the nominal to the perturbed case represented an approximate doubling of the specific intensities such as those shown in figure 7 (see ref. 47). Certain other minor additions were also made; overall, however, the increase in intensities represented an approximate doubling. This change is a reasonable approximation of the uncertainties currently existing in the radiation intensities.

UNCERTAINTY	NOMINAL	PERTURBED
AIR ABSORPTION COEFFICIENTS	WILSON & NICOLET	2 × (WILSON & NICOLET)
TRANSITION - Re_ℓ		
BICONIC	2.5×10^6	1.0×10^6
BLUNT BODY	0.45×10^6	0.2×10^6
TRANSPIRATION EFFECTIVENESS		
$\lim_{\dot{m}>>0} (q/q_o)_{CONV.}$	0	0.3
SURFACE EMISSIVITY, ϵ	0.6	0.9
CHAR SUBLIMATION TEMPERATURE AT 1 atm	3750° K	3370° K
PYROLYSIS GAS CHEMISTRY	EQUILIBRIUM	FROZEN AT DEGRADATION COMPOSITION ($T \approx 925°$ K)

Figure 18.- Some uncertainties studied.

The second uncertainty considered was the Reynolds number for boundary-layer transition from laminar to turbulent flow.[48] Since transition Reynolds numbers differ widely for blunt and for conical bodies, different values were selected for the two shapes. The nominal values shown do not represent optimism but have been obtainable in the past. The perturbed values are about a factor of 2.5 lower which is typical of the usual uncertainties in transition Reynolds numbers. Actually, the perturbed values were selected after some trial and error. In first attempts to study transition effects, Reynolds

numbers were based on displacement thickness. It was found, however, that the boundary layers on vehicles moving at hyperbolic speed were, in effect, highly cooled. Displacement thicknesses were reduced accordingly as were the Reynolds numbers based on displacement thickness. For any reasonable range of transition Reynolds numbers suggested by existing data, the flow was predicted to be laminar during nearly all of the period of entry heating and no uncertainty effects could be studied.

The next uncertainty deals with the effectiveness of ablation gases in reducing net heat transfer to the body surface. It is often considered that the net heat transfer can be reduced to zero by sufficiently large ablation or blowing rates. There is some evidence for coupled systems like ablating surfaces, however, that the net heat transfer approaches some asymptotic, nonzero value.[49] In the uncertainty study it was assumed for the perturbed case that the asymptotic value of the convective heat transfer for very large blowing rates was 30 percent of the heat transfer in the absence of blowing.

Another uncertainty is the surface emissivity which, of course, directly determines the amount of heat reradiated by the heat-shield char.[42] The nominal value was taken as 0.6 and the perturbed value was taken as 0.9. This uncertainty is the only one for which the perturbed value represents improved rather than degraded performance for the thermal-protection system.

Another uncertainty is the combination of pressure and temperature at which the heat-shield char will sublime.[50] As noted earlier, char sublimation can be encountered if the high heating rates drive the surface temperatures to sufficiently high values. A complete description of this phenomenon requires definition of the relation between pressure and temperature along which the phase change takes place; for simplicity, however, figure 18 gives only the temperature corresponding to sublimation at a pressure of 1 atmosphere. This pressure is representative of the stagnation pressure at peak heating. The nominal case represented by a temperature of 3750° K is typical of graphite sublimation characteristics. The perturbed value is 380° lower which is representative of the uncertainty in the sublimation conditions for graphitic materials.

The final uncertainty considered relates to the composition of the pyrolysis gases as they percolate through the heat-shield char. As the gases pass through the char, they are heated in accordance with the temperature gradient through the char. For the nominal calculations, it was assumed that the gas had its thermochemical equilibrium composition at each temperature and pressure. This assumption gave the gas its maximum enthalpy and thus its maximum capability to absorb heat. Some experimental evidence[39] suggests that the pyrolysis gases are not in complete equilibrium and for the perturbed case they were assumed frozen at the composition corresponding to the degradation temperature of the virgin material. For phenolic nylon, this temperature has been determined in thermogravimetric tests to be about 925° K.

The foregoing discussion is extensive but it demonstrates the logic used to select the uncertainties studied and to choose both the nominal and perturbed conditions. These properties must be chosen carefully if the perturbation analyses are to produce valid conclusions.

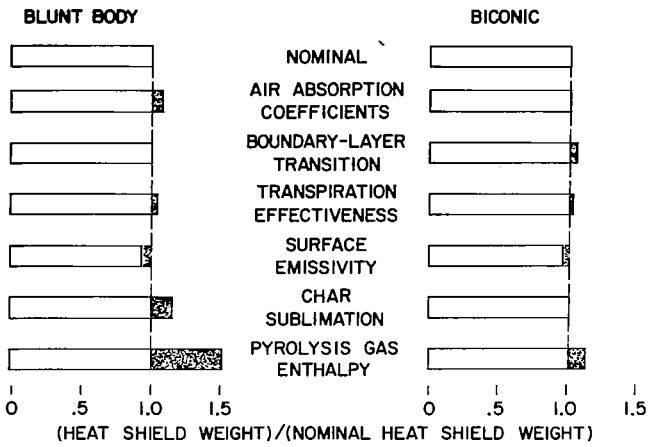

Figure 19.- Results of uncertainty analyses; V_E = 15 km/sec.

Results of the uncertainty analyses are summarized in figure 19. Effects on heat-shield weight are shown for both blunt and conical configurations.[38] The entry speed is 15 km/sec. Weights are normalized to those for the nominal conditions as shown at the top and results for each perturbation are shown below. There are two key points to be drawn from these results. First, heat-shield weights for the blunt body are more sensitive to the uncertainties in all but one case. The reason for this sensitivity is relatively simple. As noted earlier, the greater radiative heating drives the surface temperature on the blunt bodies to levels that result in char sublimation and this sublimation occurs over large areas. Any perturbation that affects the heat shield's ability to absorb heat changes this sublimation rate and thus the char erosion rate. Char erosion is a key heat-shield consumption process as discussed by Lundell, Dickey, and Jones.[41] The one exception is that shield weights for the conical configuration are more sensitive to boundary-layer transition. The sensitivity results simply because heating of the conical shape is predominantly convective while that of the blunt body is predominantly radiative.

While the uncertainties do not appear to have a large effect on heat-shield weights, it should be recognized that some of the effects could be additive. An uncertainty of 50 percent, which can result from the more important of the single uncertainties or from a combination of effects, would alter the heat-shield weight by about 400 kg. As discussed earlier, this weight can correspond to 400 metric tons of launch vehicle.

The uncertainty analyses have dealt only with the forward facing heat shield and variations in the performance of the afterbody shield were not considered. The latter shield was assumed to be made of low-density phenolic nylon (0.5 gm/cm^3). Advanced materials for the afterbody, or for that matter, for the forward face could produce significant weight savings; since each 100 kg of shield weight can represent up to 100 metric tons of launch vehicle, the return from such savings is quite important.

While the foregoing uncertainty analyses are of considerable value, they are also handicapped by the lack of experimental results that was discussed earlier. For example, the magnitudes of the basic uncertainties used in the analyses are themselves unknown and the results are directly dependent on these inputs. It is also possible that the heat-shield analysis has overlooked some important phenomena. For example, throughout the uncertainty analyses it was assumed that the thermal protection system would respond to the heating environment in an orderly fashion (that is, the surface would be removed by chemical action) and that just some of the detail characteristics were uncertain. There is another phenomenon which could be considered an

uncertainty that could result in the heat-shield behavior being anything but orderly. If thermomechanical erosion or spallation should occur (and at the heating rates discussed earlier, it is a real possibility), the heat-shield performance would be so degraded that catastrophic failure could occur.[2] In this connection all of the foregoing analyses of heat-shield performance and weight were based on the use of phenolic nylon. At the present time it is not known if phenolic nylon can withstand the radiative heat flux near 5 kW/cm^2 without spalling. Problems such as this emphasize the need for experimental results.

Facilities

The results of the uncertainty analyses confirm the need for additional research related to the heating environment and to thermal-protection systems for hyperbolic speeds. It is also apparent that knowledge of many of the key phenomena is imperfect and thus experimental work is essential. For this reason, the adequacy of existing facilities to use in this research is important.

Some of the important conditions that should be provided by the test facilities include velocity, density, enthalpy, and flow energy. The last parameter is important to the study of the nonadiabatic or energy depletion phenomenon shown to have such important effects on radiative heating. Scale is also important both to the energy depletion phenomena and to the study of materials and systems for thermal protection. For example, the nonequilibrium effects on the pyrolysis gases discussed in the previous section are importantly dependent on the time it takes these gases to traverse the char. This time is, in turn, dependent on the thickness or scale of the char. For much the same reasons, test equipment capable of essentially steady-state operation is desirable. In addition, scale, density, and velocity are all important to the study of convective heating with turbulent flow.

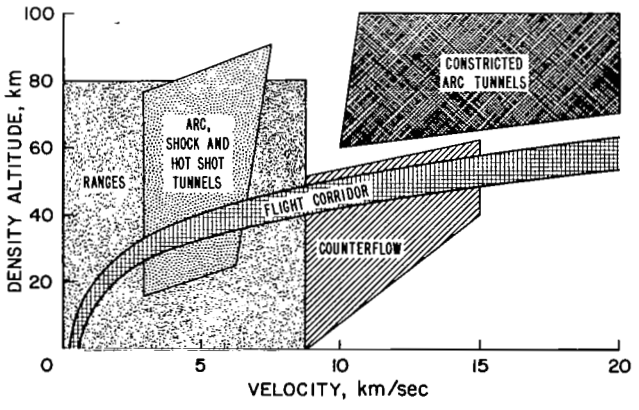

Figure 20.- Typical flight regime; $500 \leq m/C_DA \leq 1500$ kg/m^2, $G_{max} = 10$ g, $0 \leq L/D \leq 0.5$.

The desired and available test characteristics in terms of density altitude and velocity are shown in figure 20. A typical entry trajectory in these coordinates appears as a line of essentially constant velocity starting at very high altitudes and extending into the shaded flight corridor. The curve then stays within this shaded corridor as the vehicle decelerates. The approximate ranges of test conditions available for various types of test equipment are also indicated. Equipment considered includes still-air ranges with gun-launched models,[51,52] counterflow facilities which use the same launchers but fire the models in opposition to high-speed air streams,[51,52] shock tunnels,[53-55]

hotshot tunnels,[56] standard arc tunnels,[57,58] and constricted arc tunnels.[59-63] Since the new range of interest corresponds to speeds between about 11 and 18 km/sec, only the counterflow and the constricted arc tunnels provide the desired conditions. The counterflow facilities have the advantage of providing the desired densities, but they have well-known problems associated with model instrumentation and launch stresses. The constricted arcs do not have these problems and provide high test speeds but have low stream densities.

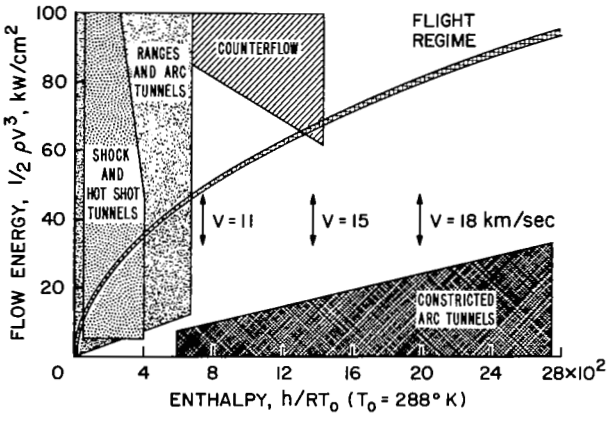

Figure 21.- Typical facility requirements for flow energy.

A corresponding comparison of desired and available test conditions in terms of flow energy and enthalpy is shown in figure 21. As noted in earlier discussions, the flow energy is the stream property particularly important to the nonadiabatic effects on radiative heating. In this case the region of interest is above the heavy curve. The range of speeds from 11 to 18 km/sec corresponds to values of the enthalpy parameter between about 700 and 2000. The counterflow facilities provide the flow energy desired but they have the problems noted earlier. In addition, the gun-launched models are necessarily quite small and scale is also important to the radiation decay problem. For example, the small models produce relatively thin shock layers. The time required for the air to traverse the shock layer is thus much less than that for a full-scale layer. The flow time is important because it is the period during which the air loses energy. With the small models, therefore, a much smaller part of the flow energy is lost by radiation. The existing constricted arcs do not provide the flow energy desired. One reason for the constricted arcs being somewhat low is that higher flow energies require higher power. As an example, the flight cases considered earlier indicated shock-layer thicknesses of about 10 cm. With an appropriately designed tunnel nozzle, it is possible that these thicknesses could be achieved with a model of about this same dimension, 10 cm in diameter. The stream should be about 2 to 2-1/2 times this diameter and thus its area would be about 500 cm^2. The constricted arcs are about 50 percent efficient in imparting the electrical energy in the stream. All of these numbers result in the guideline that the ordinate scales in figure 21 give the facility power requirements in megawatts. The required power is thus about 60 to 70 MW and the facility is thus a major one by all definitions; however, it appears essential to the development of the technology necessary to permit entry into the Earth's atmosphere at 15 to 18 km/sec.

Summary

As the foregoing material suggests, the primary research and technology problems associated with Earth entry for manned planetary missions seem to be those produced by the higher entry speeds. At these speeds, which can range

from 15 to 18 km/sec, radiative heat transfer exerts a major influence on configuration selection and on thermal protection. The problems in gasdynamics, in gas physics, and in material formulation and characterization are complex and will require considerable effort in the years to come.

The one problem not discussed in the foregoing material was that of landing. It would appear that the landing systems required for Earth return are reasonable extensions of Apollo technology since the entry vehicle weights and sizes are only moderately greater than those of the Apollo command module. There is, however, considerable research in this area related especially to providing a land landing capability for returning spacecraft. This effort covers everything from gliding parachutes, to lifting bodies, to rotors. In the time before a manned planetary mission, one of these technologies may evolve to the point where it can be applied to this mission. It should be recognized, however, that for missions as infrequent as manned planetary missions are likely to be, many of the arguments for land landing lose their significance.

The landing problem is much more important for the target planet. With this point in mind, the subject of entry and landing at the target planet will now be considered.

PLANETARY ENTRY AND LANDING

Entry Speeds

It is appropriate to open the subject of planetary entry with a discussion of the entry speeds that will probably be encountered. The definition of these speeds is not quite so difficult as it is for Earth entry. The ranges of entry speed of interest[6] are shown in figure 22 for entry directly from a transfer trajectory from Earth and for entry from a near planet orbit. Results are shown for both Mars and Venus. The range shown for direct entry is indicative of the variation over a complete cycle of opportunities. For entry from orbit, the range indicates the variation due to orbit eccentricity. The combined range of entry speeds indicated is relatively modest - from about 4 to 10 km/sec for entries from orbit and from about 7 to 13 km/sec for direct entry.

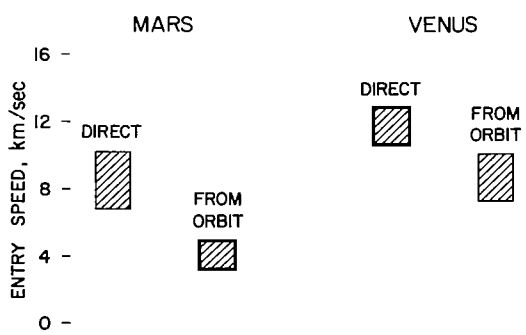

Figure 22.- Planetary entry speeds.

Atmospheres

With the range of entry speeds established the next problem is to examine the probable structure and composition of the atmospheres of the target planets. Many models of the atmospheres of Mars and Venus have been published and some measurements of atmosphere properties have been made in the last several years.[64-73] A representative range of atmospheres for Mars is shown in figure 23 in terms of the altitude-density profiles. Some models lie outside the range shown in figure 23 but the range is a reasonable one for most engineering calculations.[65,68]

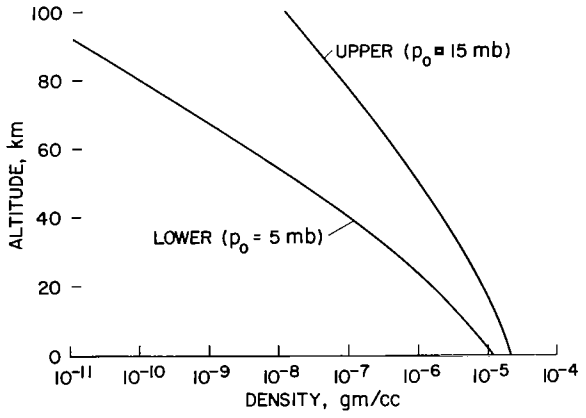

Figure 23.- Mars atmosphere models.

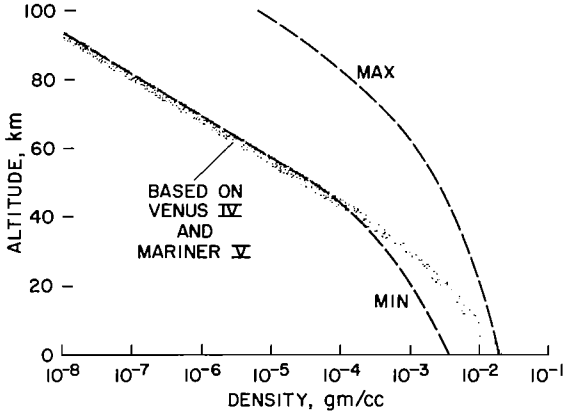

Figure 24.- Venus atmosphere models.

Corresponding information for Venus is shown in figure 24.[72] The minimum and maximum curves shown are those that existed[64,67] before data were obtained from the Russian[69,70] and American[71] missions during the 1967 opportunity. Combining some of the results of these two missions gives an estimate for the Venusian atmosphere. The estimate shown by the heavy curve in figure 24 is based on the results from Venera 4 at low altitudes and the use of the scale height from Mariner 5 to extrapolate the densities at higher altitudes.[72] It is known that there are some important differences between the results from the two missions[73]; however, the estimate shown in figure 24 will suffice for the present purposes since only corridor depth and heating will be examined for Venus.

Information defining the composition of the atmospheres of these two planets is not so complete.[67-70] It is known that large amounts of CO_2 are present in both atmospheres. The Russian results[69-70] indicate the composition of the Venusian atmosphere to be, by volume, 90-95 percent carbon dioxide, less than 7 percent nitrogen, 0.1 to 0.7 percent water vapor, and 0.4 to 0.8 percent oxygen. The estimates for the Martian atmosphere run from 100 percent carbon dioxide, to 80 percent carbon dioxide and 20 percent nitrogen or argon or their mixture, to 50 percent carbon dioxide and 50 percent argon.[68]

Entry Corridors

With some estimate of the range of atmospheres that are likely to be encountered, it is possible to estimate the characteristics of an entry

vehicle required to provide a reasonable entry corridor. Such estimates have been presented by Roberts[6] and his results are included in those summarized in figure 25 where required entry vehicle lift-drag ratios are shown as a function of the drag loading parameter, m/C_DA. The requirements correspond to an entry corridor depth of 20 km. Results are shown for entry into the Martian atmosphere at 10 km/sec and into the Venusian atmosphere at 12 km/sec which are representative of the higher direct entry speeds shown in figure 22.

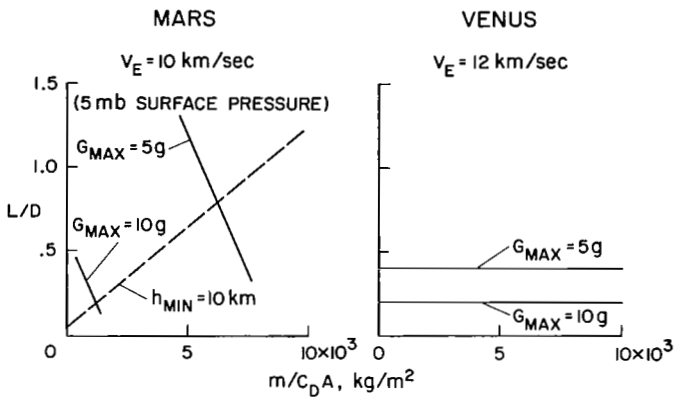

Figure 25.- Planetary entry requirements; 20-km corridor.

Results have been obtained for several different conditions. First, corridor depths were estimated for maximum accelerations for both 5 and 10 Earth g. The lift-drag ratios required for entry into the Venus atmosphere are relatively modest for either acceleration and are essentially independent of drag loading parameter (fig. 25). The lift-drag ratios required for entry into the Martian atmosphere at the same two maximum accelerations are somewhat greater and depend strongly on drag loading parameter. This dependency results from the minimum altitudes being below the tropopause and thus in a region of the atmosphere where the variation of density with altitude is not exponential. The relatively low pullout altitudes are a direct consequence of the low surface pressure considered to exist on Mars. In view of this problem, results are also shown for the lift-drag ratios required to restrict the minimum pullout altitude to 10 km. This altitude was selected to assure that no collisions would occur between the entry vehicle and possible high surface features on the planet. For larger drag loading parameters this minimum altitude is important since considerable lift is required to achieve capture of the heavier vehicles at an overshoot altitude of 30 km. Both for this restriction and when the maximum acceleration is limited to 5 g, the lift-drag ratios for Mars entries are relatively high. The selection of vehicle configurations suitable for planetary capture and providing the required characteristics indicated in figure 25 has not yet been explored in great depth.[27] It may prove to be an important area of research if atmosphere braking for planetary capture continues to be considered for these missions. In further pursuit of this point, it may seem that the values of drag loading parameter considered in figure 25 are relatively large. It should be recognized that the magnitude of this parameter depends on vehicle size. The vehicles involved in this maneuver are likely to be very large since they will contain Earth return propulsion, mission modules, Earth-entry vehicles, planetary excursion vehicles, and other miscellaneous items. Weight estimates in the hundred thousand kilogram class are typical.[14,27] In view of the extreme size of these vehicles it is questionable whether or not 10 g is an allowable acceleration. As the results in figure 25 show, lowering the acceleration to 5 g results in relatively high lift-drag ratios for Mars entries. Again, all of this discussion suggests that additional configuration research will be required in this area.[27]

Heating

The speeds for planetary entry shown in figure 22 are somewhat lower than those for Earth return, and they are close to the range for which experience exists. For these reasons, the primary heating problems to be considered are the effects of atmosphere composition on convective and radiative heating. The effects on convective heating can be estimated easily from the results of Marvin and Pope[74] and the results of such estimates are shown in figure 26.

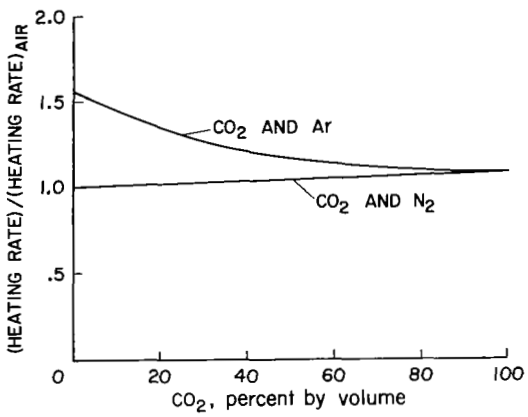

Figure 26.- Convective heating in planetary atmospheres.

The ratio between the stagnation-point convective heating rate in a planetary atmosphere to that in air is shown as a function of the percent of carbon dioxide in the planetary gas mixture. Results are shown for mixtures both of carbon dioxide and argon and of carbon dioxide and nitrogen. Presented in this form the results are independent of velocity and stream density although it is tacitly assumed, of course, that the comparisons are made at the same values of velocity and density. As discussed earlier, the atmospheres of both Mars and Venus are believed to contain somewhere between 50 and 100 percent carbon dioxide. With this composition, the results in figure 26 indicate that the convective heating will be less than 20 percent greater than that in air. This difference is relatively small compared to other uncertainties and thus no major problem is indicated in the area of convective heating.

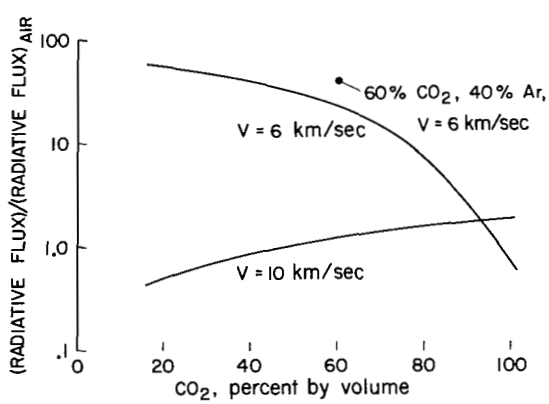

Figure 27.- Radiative heating in planetary atmospheres; CO_2/N_2 mixtures, 1-cm slab, $\rho = 1.3\times10^{-6}$ gm/cc.

Similar results for radiative heating[75,76] are shown in figure 27. Here the ratio is dependent on both density and velocity, and results are shown for a typical density. Two representative velocities and curves are presented only for mixtures of carbon dioxide and nitrogen. These results show that composition has a far greater effect on radiative heating than on convective heating. This effect is particularly great at the lower speed. In large part, however, this trend is a result of the way in which the results are presented. At 6 km/sec, the radiative heating from air is quite small, and since it forms the base for the results presented in figure 27, the ratios are large. In the CO_2/N_2 mixtures, the radiation at low speeds is due to the cyanogen radical.[77] The heating rates themselves, however, are relatively modest and well below those for 10 km/sec. At this speed, the cyanogen is dissociated and the radiation more

nearly equals that in air. It is important to recognize, however, that the curves in figure 27 apply only for mixtures of carbon dioxide and nitrogen. If the mixture is carbon dioxide and argon, then the radiative heating is greater. Only a single point is available for such mixtures and it is also shown in figure 27. The mixture is 60 percent carbon dioxide and 40 percent argon and the velocity is 6 km/sec. The heating is about twice that for corresponding conditions in nitrogen mixtures. At this speed, the primary contribution of argon is to produce higher temperatures that increase radiation from the carbon dioxide. This effect is tempered somewhat because the argon dilutes the concentration of radiating gases. No quantitative results are available for the higher speed, but at this speed the temperatures are sufficiently high that argon itself begins to radiate strongly. The radiation in CO_2/argon mixtures will be significantly greater than that in CO_2/N_2 mixtures or that in air. For these reasons, identification of argon in the atmosphere of Mars is an important problem for scientific investigation.

Another factor which tends to increase radiative heating for planetary capture is the size of the entry vehicles. As noted earlier, these vehicles are typically very large and can have relatively large nose radii. The shock layers are thus very thick and provide a large volume of radiating gas.

Landing

As noted in some of the earlier discussion, the low surface pressures believed to exist on Mars introduce problems associated with providing entry corridors sufficiently far above the mean surface to avoid collisions with possible high features. Another problem introduced by the low pressures is that of obtaining sufficient retardation from the atmosphere to permit a soft landing.[78] One way to demonstrate the magnitude of this problem is to examine the equilibrium terminal speed for entry vehicles. These speeds can be easily calculated and the results are shown in figure 28 as functions of drag loading parameter. The effect of vehicle lift-drag ratio on the terminal speed is quite small as indicated by comparison of the results for lift-drag ratios of 0 and 1. In considering these results, it should be recognized that a manned landing on a planet will probably be made with an excursion module similar in concept to the lunar module to be used in the Apollo program. For these vehicles, the weights will probably range in the tens of thousands of kilograms and the corresponding drag loading parameters will be in the range of a few thousand kg/m^2. The results in figure 28 indicate that for these drag loading parameters the terminal speed is supersonic; sonic speed for pure carbon dioxide at the estimated Martian

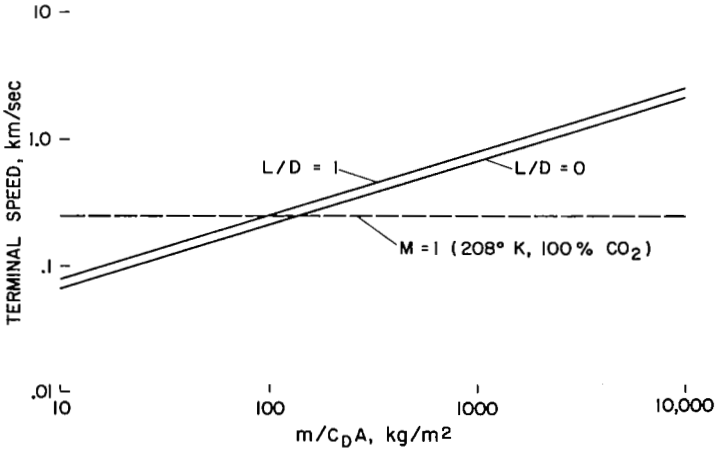

Figure 28.- Equilibrium terminal speeds for Mars; 5-mb atmosphere.

surface temperature of 208° K is shown in figure 28. If parachutes are to be used for part of the retardation, then they must be deployed at supersonic speeds. The results in figure 28 are just indicative of the problem since the parachute would necessarily be deployed well above the surface and since the entry vehicle may not reach terminal speed, especially at the higher deployment altitudes. More complete analyses of the parachute problems for Mars, including considerations such as these, have been carried out.[6,78] From these earlier analyses, results such as those shown in figure 29 can be obtained. These results are based on detailed trajectory calculations and, of course, on a number of assumptions. For example, it was assumed that the retardation

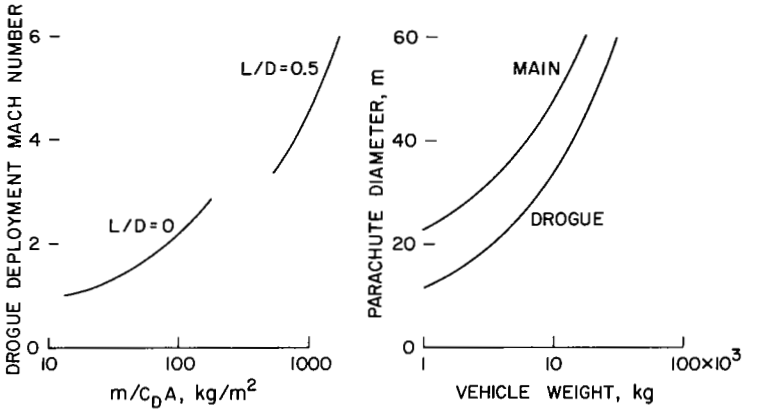

Figure 29.- Parachute requirements for Mars; landing from orbit.

system had three stages - a drogue parachute, a main parachute, and retrorockets for final touchdown. The drogue parachute was assumed to be deployed at 10 km from a vehicle in essentially level flight. (An entry vehicle with reasonable lift-drag ratio and drag loading can achieve this condition.) The drogue was considered to be sized to decelerate the vehicle to sonic speed at an altitude of 3 km. At this point, main parachute deployment was assumed and this parachute was sized to give a terminal speed of 100 m/sec. This terminal speed was chosen on the basis that the weight of the overall retardation system reaches nearly minimum when the transition from parachute to retrorocket is made at about this speed.[78] The results in figure 29 confirm that the drogue deployment Mach numbers are well into the supersonic regime; they are, in fact, about at the limit of present technology. While some parachutes have been deployed at the required Mach numbers, the parachutes were much smaller than will be required for the application being considered here. The diameters required for both the drogue and main parachutes are shown at the right of figure 29. For a vehicle weighing about 10,000 kg, the diameter of the drogue is about 35 m and the diameter of the main parachute is about 50 m. Manned excursion vehicles will probably weigh more than 10,000 kg.[79,80] Hence, the parachutes will be very large indeed and, as just noted, the combinations of size and deployment Mach number are well beyond current experience. Some of the required information could be obtained in the higher parts of Earth's atmosphere (about 35 km) by the techniques used in the Planetary Entry Parachute Program (PEPP) at NASA Langley Research Center.[81] This program is providing information for possible unmanned missions. It should also be recognized that alternates to parachutes may prove more attractive, for example, a limp paraglider. Another landing system which has some

advantages of simplicity consists of using the vehicle itself to obtain atmospheric deceleration, eliminating parachutes altogether, and using retrorockets to cancel the residual velocity after entry. Roberts[6] examined this system and found that it reduced landing payloads about 15 percent compared to a system involving two-stage parachutes and smaller rockets for impact attenuation. It will be very appropriate in the future to study such systems and their problems if efficient and reliable landing systems for use at Mars are to be evolved.

Other problems associated with landing on Mars include the need to know more about the environment of the landing site. For example, winds up to 135 km/hr have been inferred from movements of the yellow dust clouds, and even higher velocities have been suggested in order to explain the entrainment of the dust particles by the Martian atmosphere.[68] The existence of such winds will obviously have a major effect on the design of the landing system. Another important consideration is the character of the surface. If the landing site is relatively unknown, then the landing vehicle may need a capability for hovering and translation. This capability is relatively expensive since the fuel necessary to hover and translate for 10 minutes will more than double the weight of the landing vehicle. Both of these discussions suggest the need for extensive unmanned exploration of the Martian atmosphere and surface prior to any manned missions. Indeed, it can be argued that the need is greater than for lunar exploration since our knowledge of Mars is less complete and the environment is more complex than that of the Moon.

Summary

As the foregoing section suggests, the landing system design for Mars missions is one of the major problems introduced by the characteristics of the atmospheres now believed to exist on Mars and Venus. No detailed consideration has been given to landing on the surface of Venus since the Russian results[69,70] indicate surface conditions that appear to make a manned landing academic. It is difficult to see how men and their landing vehicle could be protected from the high surface temperature (533° K) and the high surface pressure (15 to 22 atm) given by the Russian measurements. Even if such protection were technically feasible, the high surface pressure has major effects on the takeoff propulsion requirements due to drag losses and to thrust losses from high back pressures on the rocket nozzle. Simple estimates suggest that the takeoff weight required to return a two-man, 3,000-kg vehicle to Venusian orbit ranges from about 350,000 to 700,000 kg. These weights are about two to four times the corresponding weights for orbiting Earth. Apparently, the Russian probe was also lofted by the atmosphere during its descent which suggests the existence of significant winds or atmosphere turbulence on Venus. These winds would also be important to the design of a landing vehicle. The principal problems, however, would appear to be in the design of environmental control systems for use on the surface and in the design of the takeoff propulsion system. Fortunately, however, these two technological areas do not fall within the scope of the present paper.

While the landing problem has been emphasized, there are at least two other problems associated with planetary entry that should not be ignored.

One of these is associated with capture. The corridor depths available to a vehicle of typical characteristics are reasonable in terms of experience at Earth.[82] For the planetary capture maneuver, however, there will be no ground-based tracking or other assistance for guidance and navigation during approach. It is believed that this problem deserves further attention.

Another problem that was mentioned is related to the heating during planetary capture. Should significant amounts of argon be present in the Martian atmosphere, then the radiative heating experienced at the capture entry speeds of 10 or 11 km/sec could be increased significantly. Designing a thermal-protection system for the very large vehicles involved (weights of the order of 100,000 kg) and subject to intense radiative heating could prove to be a formidable problem.

It is also apparent that better knowledge of the Martian atmosphere will tend to resolve many of the problems just discussed. For this reason, initial experiments designed for this objective perhaps along the lines employed by the Russians for Venus or along the lines suggested by Seiff[83] for Mars would seem to be appropriate. Recently, Seiff[84] used the techniques he and his colleagues[85] evolved along with results obtained from the Venera 4 mission to extract additional information on the composition and structure of the Venusian atmosphere.

CONCLUDING REMARKS AND RECOMMENDATIONS

In this paper, some of the research problems associated with atmosphere entry and landing for manned planetary missions have been assessed. Two sets of problems were considered, those associated with Earth return and those associated with capture and landing at the target planet.

For manned planetary missions the maximum entry speeds at Earth return range from 15 to 18 km/sec. For these entry conditions, the principal problems are associated with entry heating and with providing thermal protection from the heating environment. This environment is characterized by convective heating rates about three times greater than those for Apollo entry conditions, and for blunt entry vehicles, it is also characterized by radiative heating rates more than an order of magnitude greater. For blunt bodies, the radiative rates range from 5 to 10 kW/cm^2. While these rates are impressive, they are about an order of magnitude less than those potentially available from the energy contained in the incident flow. The reduction estimated in the radiative rates results from nonadiabatic cooling in the hot gas cap. The nonadiabatic processes are thus a new phenomenon that must be considered in heating analyses for hyperbolic entry. Since nonadiabatic cooling plays a major role in determining heating rates, there is a need for further study of this phenomenon, and it is significant that at the present time there does not exist a definitive set of experimental results that provide the necessary confirmation of theoretical methods on which heating analyses such as the present one are based. Basic experimental studies of radiative heating from flows with nonadiabatic losses are thus very important in establishing methods for analyzing heating at hyperbolic speeds.

Previous investigators have shown that it is possible to avoid excessive radiative heating by the use of a conical entry vehicle. The need of this approach for manned planetary missions and thus the need for developing a new class of entry vehicles depends strongly on the magnitude of the radiative heating for blunt bodies. For this reason, establishing and evaluating the required methods of heating analysis are objectives of major significance.

The severity of the entry heating has a direct effect on the design of thermal-protection systems. Analyses show that uncertainties in the heating environment and in the response of heat-shield materials to the environment result in 50 percent uncertainties in the required weight of thermal-protection systems. Of greater importance, however, is the almost total lack of experience with the response of heat-shield materials subjected to radiative fluxes of the level possible, namely, 5 to 10 kW/cm^2. The ability of appropriate materials to withstand these fluxes without catastrophic failures such as spallation must be established before the results of analyses such as the present one can be accepted with confidence. For this reason, the need for definitive experiments in this area is every bit as great as it is in the case of radiative heating. Once this key step is made, an orderly program of advancing the necessary technology can be developed. This program should include material formulation, characterization, and testing along with the analysis of thermal-protection system response. From this program will evolve the advanced materials and methods of analysis suitable for application to manned planetary missions.

Other technologies associated with entering the Earth's atmosphere will also require some advancement prior to any manned planetary mission. The present review suggests that in most areas other than the two just discussed, the required advances can be expected from normal evolutionary growth.

The problems associated with capture and landing at the target planets were also examined. The entry speeds associated with missions to Mars and Venus are relatively modest, not exceeding about 12 to 13 km/sec. At these speeds, entry heating is not excessive even with some increases due to the effects of composition of the planetary atmospheres. The primary thermal-protection problems are associated with the size of the entry vehicles. These vehicles are especially large if atmosphere braking is to be used for capture at the planet. Perhaps the key problem examined for planetary capture and landing is that of obtaining the retardation desired from the tenuous atmosphere believed to exist on Mars. Analyses suggest the need for deploying very large parachutes at supersonic speeds. The technology required is indicated to be well beyond current experience. Parachute tests in the upper parts of the Earth's atmosphere, along the lines currently being pursued in support of unmanned missions, are suggested as a logical step in the evolution of the required parachute technology.

Many of the problems examined for planetary capture and landing would be eased with improved knowledge of the planetary environment. It is suggested

therefore that unmanned missions to define the atmosphere composition, structure, and winds and to define the surface characteristics are a key step in preparing for manned planetary landing missions.

Ames Research Center
National Aeronautics and Space Administration
Moffett Field, Calif., 94035, Jan. 15, 1968
124-07-01-18-00-21

REFERENCES

[1]Allen, H. J., "Problems in atmosphere entry from parabolic orbits," *Conference on Aeronautical and Space Engineering* (Nagoya, Japan, 1960).

[2]Allen, H. J., "Some problems of planetary atmosphere entry," J. Roy. Aero. Soc. (Jan. 1968).

[3]Seiff, A., "Atmosphere entry problems of manned interplanetary flight," *AIAA and NASA Conference on Engineering Problems of Manned Interplanetary Exploration* (New York, 1963).

[4]Seiff, A., "Developments in entry vehicle technology," AIAA Paper 64-528.

[5]Seiff, A., "Current and future problems in Earth and planetary atmosphere entry," AIAA Paper 67-803.

[6]Roberts, L., "Atmosphere entry in the post-Apollo era," *1967 Heat Transfer and Fluid Mechanics Institute* (La Jolla, Calif., 1967).

[7]Syvertson, C. A. and Dennis, D. H., "Trends in high-speed atmospheric flight," AIAA Paper 64-514.

[8]Syvertson, C. A. and Swenson, B. L., "Lifting entry for manned planetary missions," *Proceedings of the ASSET/ALRT Symposium* (Miami, Fla., 1965), pp. 1411-1448.

[9]Anderson, J. L. and Swenson, B. L., "A parametric analysis of three vehicle shapes for use as planetary return vehicles," AIAA Paper 68-152.

[10]McCarthy, J. F., Jr. and Hanley, G. M., "Earth entry at hyperbolic velocities," AIAA Paper 68-153.

[11]Ehricke, K. A., "A study of manned planetary missions," *Proceedings of the Symposium on Manned Planetary Missions. 1963/1964 Status.* NASA TM X-53049, Part 1 (1964), pp. 7-74.

[12]Martin, B. P., "Manned interplanetary missions," *Proceedings of the Symposium on Manned Planetary Missions. 1963/1964 Status.* NASA TM X-53049, Part 2 (1964), pp. 75-140.

[13]Dixon, F. P., "The Empire dual planet flyby mission," AIAA Engineering Problems of Manned Interplanetary Missions, Oct. 1963, pp. 3-18.

[14]Jones, A. L. and McRae, W. V., "Manned Mars landing and return mission study. Volume 1 - Condensed summary. Final Rept.," NASA CR-57012 (1964).

[15]Sohn, R. L., ed., "Manned Mars landing and return mission," TRW Space Technology Laboratories Rept. 8572-6011-RU-000, Vol. 1 (March 1964) (Contract No. NAS2-1409).

[16]Wong, T. J. and Anderson, J. L., "A preliminary study of spacecraft for manned Mars orbiting and landing missions," SAE Paper 857B (1964).

[17]Dugan, D. W., "A parametric study of mass ratio and trajectory factors in fast manned Mars missions," NASA TN D-2225 (1965).

[18]Ross, S., ed., "Planetary flight handbooks," Vol. 3, Parts 1-3, NASA SP-35 (1963).

[19]Sohn, R. L., "Venus swingby mode for manned Mars missions," J. Spacecraft Rockets 1(5), 565-567, (1964).

[20]Hornby, H., "Ames Research Center Mars mission studies summary, Part 7," *Proceedings of the Symposium on Manned Planetary Missions, 1963/1964 status*. NASA TM X-53049 (1964).

[21]Hollister, W. M. and Prussing, J. E., "Optimum transfer to Mars via Venus," AIAA Paper 65-700.

[22]Deerwester, J. M., "Initial mass savings associated with the Venus swingby mode of Mars round trips," AIAA Preprint 65-89.

[23]Deerwester, J. M. and D'Haem, S. M., "Systematic comparison of Venus swingby mode with standard mode of Mars round trips," AIAA Preprint 67-27.

[24]Manning, L. A., "Comparison of several trajectory modes for manned and unmanned missions to Mercury: 1980-2000," AIAA Preprint 67-28.

[25]Cicolani, L. S., "Interplanetary midcourse guidance using radar tracking and on-board observation data," NASA TN D-3623 (1966).

[26]Page, W. A. and Arnold, J. O., "Shock-layer radiation of blunt bodies at reentry velocities," NASA TR R-193 (1964).

[27]Hearne, L. F., et al., "Study of heat shielding requirements for manned Mars landing and return missions," NASA CR-57549 (1964).

[28]Page, W. A., Compton, D. L., Borucki, W. J., Ciffone, D. L., and Cooper, D. M., "Radiative transport of nonisothermal shock layers," *AIAA Third Thermal Physics Conference* (Los Angeles, 1968).

[29]Yoshikawa, K., "Analysis of radiative heat transfer for large objects at meteoric speeds," NASA TN D-4051 (1967).

[30]Hoshizaki, H. and Wilson, K. H., "Convective radiative heat transfer during superorbital entry," AIAA J. 5(1), 25-35 (1967).

[31]Wilson, K. H. and Nicolet, W. E., "Spectral absorption coefficients of carbon, nitrogen and oxygen atoms," Lockheed Missiles and Space Company Rept. LMSC-4-17-66-5 (November 1966).

[32]Chin, J. H., "Radiation transport for blunt-body flows including the effects of lines and ablation layer," NASA CR-73223 (1968).

[33]Allen, H. J., Seiff, A., and Winovich, W., "Aerodynamic heating of conical entry vehicles at speeds in excess of Earth parabolic speed," NASA TR R-185 (1963).

[34]Seiff, A. and Tauber, M., "Minimization of the total heat input for manned vehicles entering the Earth's atmosphere at hyperbolic speeds," NASA TR R-236 (1966).

[35]Shapland, D. J., "Preliminary design of a Mars-mission Earth reentry module," Lockheed Missiles and Space Company Rept. 4-57-64-1 (February 1964) (Contract No. NAS9-1702).

[36]Shapland, D. J., et al., "Study of manned vehicles for entering the earth's atmosphere at hyperbolic speeds," Lockheed Missiles and Space Company Rept. 4-05-65-12 (November 1965) (Contract No. NAS2-2526).

[37]Shapland, D. J. and Munroe, W. F., "A comparative design analysis of three configurational families for manned earth entry at hyperbolic speeds," AIAA Preprint 66-489.

[38]Coleman, W. D., Lefferdo, J. M., Hearne, L. F., and Vojvodich, N. S., "A study of the effects of environmental and ablator performance uncertainties on heat shielding requirements for blunt and slender hyperbolic entry vehicles," AIAA Preprint 68-154.

[39]Vojvodich, N. S., "Hypervelocity heat protection - A review of laboratory experiments," *Ablative Plastics Symposium, American Chemical Society* (1968).

[40]Lundell, J. H., Wakefield, R. M., and Jones, J. W., "Experimental investigation of charring ablative material exposed to combined convective and radiative heating," AIAA J. 3, 2087-2095 (1965).

[41]Lundell, J. H., Dickey, R. R., and Jones, J. W., "Performance of charring ablative materials in the diffusion controlled surface combustion regime," AIAA Preprint 67-328.

[42]Pope, R. B., "Measurements of the total surface emittance of charring ablators in arc-heated streams," AIAA J. 5(12), 2285-2286 (1967).

[43]Parker, J. A., Winkler, E. L., Miles, B. H., and Sonnabend, L. F., "The effects of molecular structure on the thermochemical properties of phenolics and related polymers," NASA TR R-276 (1967).

[44]Dickey, R. T., Lundell, J. H., and Parker, J. A., "The development of polybenzimadizoles composites as ablative heat shields," *Ablative Plastics Symposium, American Chemical Society* (1968).

[45]Strouhal, G., Curry, D. M., and Janney, J. M., "Thermal protection system performance of the Apollo command module," *AIAA/ASME Seventh Structures and Materials Conference* (Cocoa Beach, Fla., 1966), pp. 184-200.

[46]Kotanchik, J. N. and Erb, R. B., "The design of ablative thermal protection systems," *Seventh International Aeronautical Congress* (Paris, France, 1965).

[47]Hearne, L. F., Coleman, W. D., Lefferdo, J. M., Gallagher, L. W., and Chin, J. H., "A study of the effects of environmental and ablator performance uncertainties on heat shielding requirements for hyperbolic entry vehicles," NASA CR-73224 (1968).

[48]Wilkins, M. E. and Tauber, M. E., "Boundary layer transition on ablating cones at speeds up to 7 km/sec," AIAA J. 4(8), 1344-1348 (1966).

[49]Vojvodich, N. S. and Pope, R. B., "The Influence of ablation on stagnation region convective heating for dissociated and partially ionized boundary-layer flows," *Proceedings of the Heat Transfer and Fluid Mechanics Institute* (Stanford Univ. Press, 1965), pp. 114-137.

[50]Krieger, F. J., "The thermodynamics of the graphite-carbon vapor system," Rand Corporation Memo RM 3326-1-PR (December 1965).

[51]Seiff, A., "A progress report on the Ames hypervelocity free-flight facilities and some current research problems being studied in them," AIAA Preprint 63-162.

[52]Anon., "Research facilities summary. Vol. I - Guns and ranges," Ames Research Center, Moffett Field, Calif. (December 1965).

[53]Hiers, R. S. and Loubsky, W. J., "Effects of shock-wave impingement on the heat transfer on a cylindrical leading edge," NASA TN D-3859 (1967).

[54]Loubsky, W. J., Hiers, R. S., Jr., and Stewart, D. A., "Performance of a combustion driven shock tunnel with application to the tailored-interface operating condition," *Third Conference on Performance of High Temperature Systems* (Pasadena, Calif., 1964).

[55]Loubsky, W. J. and Reller, J. O., Jr., "Analysis of tailored-interface operation of shock tubes with helium driven planetary gases," NASA TN D-3495 (1966).

[56]Griffith, B. J. and Weddington, E. D., "Recent refinements and advancements of hypersonic testing techniques in the 100-inch tunnel F of the Von Karman Gas Dynamics Facility," *Proceedings of the Fourth Hypervelocity Techniques Symposium* (Arnold Engineering Development Center, Arnold Air Force Station, 1965).

[57]Wick, B. H., "Ablation characteristics and their evaluation by means of arc jets and arc radiation sources," *Seventh International Aeronautical Congress* (Paris, France, 1965).

[58]Gowen, F. E., Lundell, J. H., and Wick, B. H., "Facilities for simulating combined convective and radiative entry-heating environments," *13th Annual Institute of Environmental Sciences Technical Meeting and Equipment Exposition* (Washington, D. C., 1967).

[59]Shepard, C. E., Watson, V. R., and Stine, H. A., "Evaluation of a constricted-arc supersonic jet," NASA TN D-2066 (1964).

[60]Shepard, C. E. and Watson, V. R., "Performance of a constricted-arc discharge in a supersonic nozzle," AIAA Preprint 63-380.

[61]Stine, H. A., "The hyperthermal supersonic aerodynamic tunnel," *International Symposium on High Temperature Technology* (Asilomar, Calif., 1963); Butterworths, Washington, D. C., pp. 85-104 (1964).

[62]Dennis, P. R., Gates, D. W., Smith, C. R., and Bond, J. B. (Compilers and Editors), "Plasma jet technology," NASA SP-5033 (1965).

[63]Shepard, C. E., Ketner, D. M., and Vorreiter, J. W., "A high enthalpy plasma generator for entry heating simulation," *13th Annual Institute of Environmental Science, Technical Meeting and Equipment Exposition* (Washington, D. C., 1967).

[64]Kaplan, L. D., "A preliminary model of the Venus atmosphere," JPL TR-32-379 (Contract No. NAS7-100) (December 12, 1962).

[65]Levin, G. M., Evans, D. E., and Stevens, V., eds., "NASA engineering models of the Mars atmosphere for entry vehicle design," NASA TN D-2525 (1964).

[66]Evans, D. E., Pitts, D. E., and Kraus, G. L., "Venus and Mars nominal natural environment for advanced manned planetary mission programs," NASA SP-3016 (1967).

[67]Koenig, L. R., Murray, F. W., Michaux, C. M., and Hyatt, H. A., "Handbook of the physical properties of the planet Venus," NASA SP-3029 (1967).

[68]Michaux, C. M., "Handbook of the physical properties of the planet Mars," NASA SP-3030 (1967).

[69]Anon., "Venus 4 underscores U. S. lag," Aviation Week and Space Technology (October 23, 1967), p. 26.

[70]Kuzmin, A. D., "The atmosphere of Venus from modern data," *COSPAR Meeting*, Tokyo, Japan, May 1968.

[71]Anon., "Mariner V Venus 1967 encounter press conference," Transcript 9837, Polk Court Reporters, Los Angeles, Calif. (October 23, 1967).

[72]Reese, D. E. and Swan, P. R., "Venera 4 probes atmosphere of Venus," Science 159 (3820), 1228-1230 (1968).

[73]Jastrow, R., "The planet Venus," Science 160(3835), 1403-1410 (1968).

[74]Marvin, J. G. and Pope, R. B., "Laminar convective heating and ablation in the Mars atmosphere," AIAA J. 5(2), 240-248 (1967).